Earth and Environmental Sciences

Biophenomena

Absolute flux measurements for IR spectromicroscopy
Martin, M.C., K. Knutsen, W.R. McKinney

Catalysis of PAH biodegradation by humic acid shown in synchtrotron infrared studies
Holman, H.-Y., K. Nieman, D.L. Sorensen, C.D. Miller, M.C. Martin, T. Borch, W.R. McKinney, R.C. Sims

Investigation of interfacial chemistry of microorganisms
Ingram, J.C., D.E. Cummings, H.-Y. Holman, M.Downing

New IR microscope and bench installed at BL 1.4
Martin, M.C., H.-Y. Holman, W.R. McKinney

Novel molecular mechanisms of disease susceptibility in plants—an FTIR study of *Arabidopsis thaliana*
Raab, T.K., J. Vogel, S. Somerville

Spatial distribution of bacteria on basalt using SR-FTIR
Kauffman, M.E., H.-Y. Holman, R.M. Lehman, M.C. Martin

SR-FTIR study of bacteria-water interactions: Acid-base titration and silification experiments
Yee, N., L.G. Benning, M.J. Tobin, K.O. Konhauser

Synchrotron infrared spectromicroscopy as a novel bioanalytical microprobe for individual living cells: Cytotoxicity considerations
Holman, H.-Y., K.A. Bjornstad, M.P. McNamara, M.C. Martin, W.R. McKinney, E.A. Blakely

Absolute Flux Measurements for IR Spectromicroscopy

Michael C. Martin[a], Kelly Knutsen[b] Wayne R. McKinney[a]
[a] Advanced Light Source Division, Lawrence Berkeley National Laboratory, Berkeley, CA 94720
[b] Dept. of Chemistry, University of California, Berkeley, CA 94720

1. INTRODUCTION

Measurements of the effects of exposure to IR light at the spectromicroscope at beamline 1.4.3 has necessitated an estimate of the absolute flux levels in the IR optical bench and in the microscope. We calculated the IR flux levels from both a thermal source and the ALS, and compared them to measurements taken at the beamline. We find a self consistent picture which can be used to estimate the absolute exposure to cells and bacteria which are examined in the IR microscope.

2. EXPERIMENTAL

The thermal ("globar") source in the Nicolet 760 IR bench was measured with a disappearing filament style optical pyrometer to have a brightness temperature of ~1343K. This allowed us to calculate the "greybody power" emitted by the filament, using the emissivity of tungsten. We also measured the output of the thermal source with a Molectron PowerMax 500D with a 19 mm dia. PM10V1 detector. To measure ratios of light both before and after the bench and the microscope a more sensitive mid IR detector was needed so we employed a T3-09 9mm dia. energy detector, and a 200 Hz chopper. We also calculated the power of the synchrotron beam using the standard bending magnet formulae. The table below summarizes our results. Unless enumerated otherwise the numbers are in watts. Bold numbers are experimental data, others are calculations or estimates.

Greybody power	1.70E-04	**0.0479**	Synchrotron Power	3.73E-02
1 to 20 microns			1 to 20 microns	
1 mm^2, 0.0064 str, 1343 K			10 x 40 mr, 1.9 GeV, 4.81 m	
Real emitting area, mm^2	100	1	Beamline coupling loss	0.333
			20 out of 40 mr * 0.67 diamond	
Bench efficiency	0.372	0.372	Bench efficiency	0.372
Chopped Energy Detector			Chopped Energy Detector	
15.9/42.7			**15.9/42.7**	
Microscope Vignetting	0.1677	0.1677	Microscope Vignetting	1
Chopped Energy Detector				
1.5/15.9 * 12^2/9^2				
Microscope efficiency	0.225	0.225	Microscope efficiency	0.225
0.6/(1.5*12^2/9^2)			**0.6/(1.5*12^2/9^2)**	
Chopped Energy Detector			Chopped Energy Detector	
Power at sample	2.39E-04	6.72E-04	Power at Sample	1.04E-03
Greybody			Synchrotron	
Ratio of Synch/Greybody	**2**		Peak Power at Sample	5.20E-02
by MCT in Microscope			Synchrotron (*50)	
Ratio from this work	1.55		for 2ns/40ps	

3. RESULTS AND DISCUSSION

Starting from two calculations, and one measurement the table precedes from top to bottom from the two sources, thermal and synchrotron to the sample. At each step, there were many factors to consider. For example, the long depth of field of the synchrotron source means that all 40 horizontal mr of beam is not coupled into the microscope, and the synchrotron beam has a diamond window loss which the thermal beam does not. Moreover, the synchrotron beam has been carefully moved from the center of the optical axis so that it is not vignetted by the special coating in the center of the beam splitter in the optical bench, and the microscope optics have been adjusted to optimally transmit the synchrotron beam. This requires that the vignetting ratios for the two cases be different. We have done our best to honestly estimate the various factors, and measure them where feasible without significant disassembly of the beamline optics.

The final results are satisfying in that the ratio of the total synchrotron to thermal flux (1.55) that we get from our careful combination of theoretical and experimental measurements matches well within the error of our methods the ratio (2.0) we measure by comparing the two sources directly with the LN_2-cooled MCT detector in the microscope. The brightness advantage of the synchrotron (>100) is also verified. The overall error in the estimates is well represented by the factor of 2.8 between the two methods for estimating the power of the thermal source. The continuous power at the microscope integrated from 400 to 10000 cm^{-1} is estimated to be approximately 1 mW, and the peak power at the top of an ALS pulse to be fifty times (2 nsec / 40 psec) that, or 50 mW.

ACKNOWLEDGEMENTS

This work was performed with support by the Directors, Office of Energy Research, and Basic Energy Sciences, Materials Science Division, of the United States Department of Energy under Contract No. DE-AC03-76SF00098.

REFERENCES

1. Michael C. Martin, Nelly M. Tsvetkova, John H. Crowe, and Wayne R. McKinney, "Negligible sample heating from synchrotron infrared beam," Applied Spectroscopy, **55**(2), 111-113 (2001).

2. Hoi-Ying N. Holman, Michael C. Martin, Eleanor A. Blakely, Kathy Bjornstad, and Wayne R. McKinney, "IR spectroscopic characteristics of cell cycle and cell death probed by synchrotron radiation based Fourier transform IR spectromicroscopy," Biopolymers (Biospectroscopy), **57**[6], 329-335 (2000).

3. Hoi-Ying N. Holman, Kathleen A. Bjornstad, Morgan P. McNamara, Michael C. Martin, Wayne R. McKinney, and Eleanor A. Blakely, "Synchrotron Infrared Spectromicroscopy as a Novel Bioanalytical Microprobe for Individual Living Cells: Cytotoxicity Considerations," Journal of Biomedical Optics 2002, *In Press.*

Principal investigator: Michael C. Martin, Advanced Light Source Division, LBNL, 510-495-2231, MCMartin@lbl.gov

Catalysis of PAH Biodegradation by Humic Acid Shown in Synchrotron Infrared Studies

Hoi-Ying N. Holman,[1] Karl Nieman,[2] Darwin L. Sorensen,[2] Charles D. Miller,[3] Michael C. Martin,[4] Thomas Borch,[5] Wayne R. McKinney,[4] and Ronald C. Sims[2]
[1]Center for Environmental Biotechnology, Lawrence Berkeley National Laboratory, Berkeley, CA 94720
[2]Utah Water Research Laboratory, Utah State University, Logan, UT 84321
[3]Biology Department, Utah State University, Logan, UT 84321
[4]Advanced Light Source Division, Lawrence Berkeley National Laboratory, Berkeley, CA 94720
[5]Center for Biofilm Engineering, Montana State University, Bozeman, MT 59717

INTRODUCTION

Humic acids (HAs) are complex organic molecules produced by the decomposition of plant and animal remains in soils. The surfactant-like micellar microstructure of HA is thought to accelerate the degradation of polycyclic aromatic hydrocarbons (PAHs) by enhancing PAH solubility, thereby increasing the PAH bioavailability to microorganisms. Despite abundant evidence that HA is important in the bioremediation of several anthropogenic pollutants, its role in the detoxification of PAHs by microbes remains uncertain.

Previous inconclusive results motivate a novel approach to the study of this important biogeochemical process. We used SR-FTIR spectromicroscopy to examine the effects of soil HA on biodegradation of the model PAH pyrene in the presence of a colony of Mycobacterium sp. JLS, on a mineral surface in an unsaturated environment. Infrared spectra measured during the onset and progress of biodegradation constitute the first microscopic study of this process to be made in real time.

PROCEDURE

SR-FTIR spectra were obtained at ALS BL1.4.3 from samples of M. sp. JLS as they degraded pyrene on magnetite surfaces, with and without the addition of Elliott Soil Humic Acid (ESHA). The pyrene-degrading microorganism M. sp. JLS is a gram-positive, rod-shape bacterium (GenBank accession no. AF387804); our samples were recently isolated from PAH-contaminated soil at the Libby Groundwater Superfund Site in Libby, Montana, USA. Our mineral substrates were freshly cleaved and sonicated surfaces of small chips (less than 1 cm in diameter) of magnetite rock from Minerals Unlimited of Ridgecrest, CA.

The time-dependent pyrene biodegradation experiments were began by adding 2.5 ml of cell suspension (~1.5 × 108 cells/milliliter) of M. sp. JLS onto the prepared magnetite chips. A custom IR microscope-stage mini-incubator was used to maintain the proper growth conditions for M. sp. JLS, while allowing *in situ* FTIR spectromicroscopy measurements. For abiotic controls, no M. sp. JLS was applied. Non-overlapping IR spectral markers were selected to monitor each component.

RESULTS

Figure 1 summarizes the time series of infrared spectra obtained by repeatedly measuring the same location on each pyrene-coated sample for more than a month. Since the sample surface is different for each experiment, the absolute value of absorbance can vary. However by

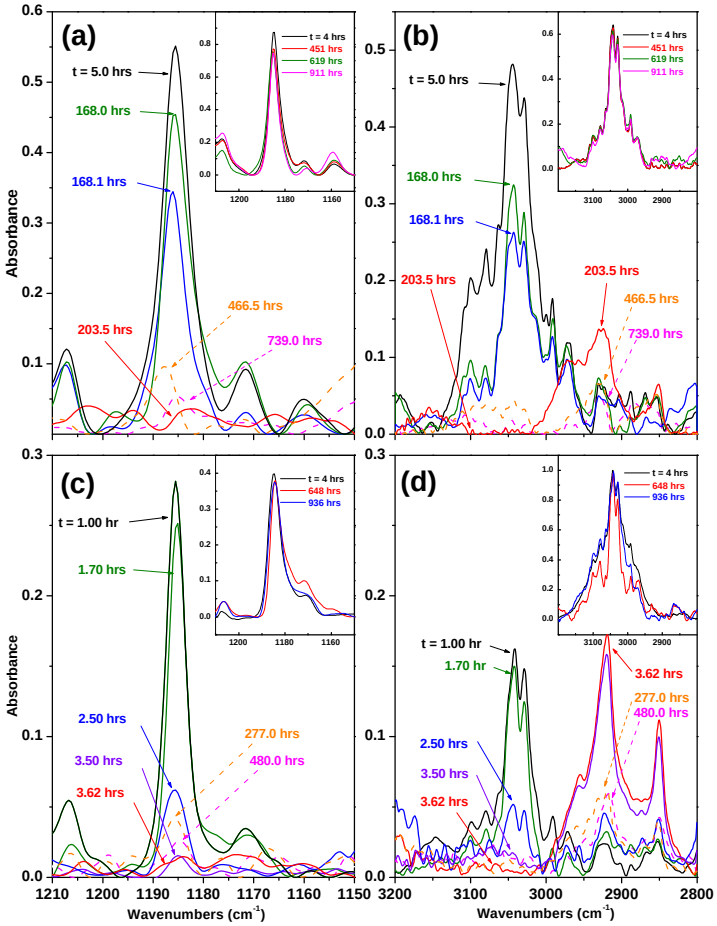

Figure 1. Time series of SR-FTIR absorption bands corresponding to pyrene and biomass formation following the degradation of pyrene by Mycobacterium sp. JLS on magnetite surfaces. Panels (a) and (b) are without ESHA; panels (c) and (d) are with ESHA. (a) and (c) show a pyrene absorption band at 1185 cm^{-1}. (b) and (d) show a pyrene doublet at 3044 and 3027 cm^{-1} and biomass IR absorption at 2921 and 2850 cm^{-1}. Inserts are abiotic control experiments.

monitoring the same position on each sample individually, the changes in absorption are quantitative. Over a similar period, the infrared spectra obtained from samples free of pyrene did not show statistically significant changes.

For samples without ESHA, pyrene biodegradation starts very slowly, and about 168 hours elapse before significant changes are observed. Biodegradation then proceeds quickly, and all the observed pyrene is completely degraded within the next 35 hours. As the pyrene peaks in the spectra disappear, we observe an increase in the biomass IR absorption peaks, implying concurrent biomass formation during the consumption of pyrene (Fig. 1, panels (a) and (b)). By contrast, the biodegradation of pyrene on samples with ESHA begins almost immediately (~1 hour) after the introduction of M. sp. JLS (Fig. 1, panels (c) and (d)). The degradation of the observed pyrene is complete by the fourth hour. Again we detect an increase in biomass absorption during the later stage of the pyrene degradation, which implies that biomass formation is concurrent with the consumption of pyrene.

Figure 2 displays pyrene concentration and biomass versus time under three different conditions, as measured by associated spectral absorbances normalized to remove surface effects as described above. Abiotic results show that pyrene remains on the mineral surface, with only slow removal mechanisms. Pyrene degradation by M. sp. JLS without ESHA did not proceed until ~ 170 hours after the introduction of the bacteria, followed by a rapid decrease of pyrene and a rapid increase of biomass within the next thirty-five hours, as described earlier. After the pyrene was depleted the biomass signal significantly decreased, presumably as the M. sp. JLS bacteria transformed themselves into ultramicrocells, a starvation-survival strategy commonly observed among bacteria in oligotrophic environments. In the presence of ESHA, pyrene biodegradation begins within an hour and the observed pyrene is depleted by the end of the fourth hour, with a concurrent increase of biomass. It is likely that the water-insoluble pyrene is solubilized into cores of ESHA pseudo-micelles and therefore becomes available for bacterial consumption.

Over longer times, IR absorption bands of pyrene on magnetite surfaces showed a slight increase and decrease. The increase is probably due to pyrene diffusing from pyrene trapped in

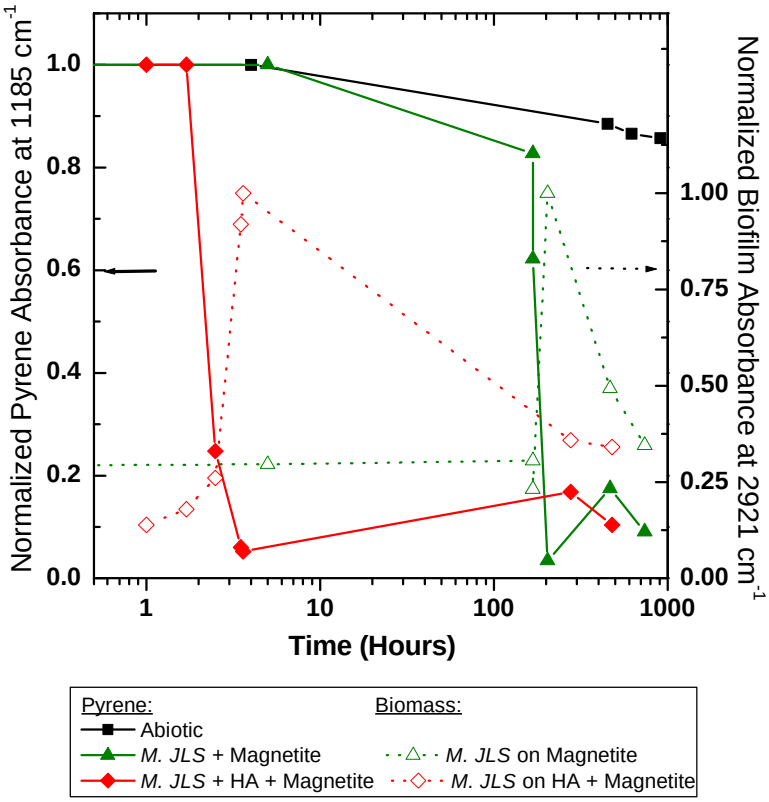

Figure 2. Summary of IR results showing that pyrene degradation occurs much faster when ESHA is present (note the log scale on the time axis). The color scheme is black for abiotic, green for biotic without ESHA, and red for biotic with ESHA. The solid lines correspond to pyrene and the dotted lines correspond to the biomass.

micropores of the magnetite and/or neighboring surfaces of higher pyrene concentration. Thus the first wave of rapid depletion of pyrene by M. sp. JLS set up a diffusion gradient from the pyrene-containing micropores toward the bacterial colony, leading to a subsequent small increase in pyrene concentration. For the surface containing ESHA, the biomass remained almost constant over a period of more than 200 hours, indicating that the flux of pyrene from the micropores was sufficient to maintain the bacterial colony. For the surface free of ESHA, there is little evidence of the presence of a quasi-steady state biomass.

DISCUSSION

Our results have significant implications for the bioremediation of contaminated soils. In many PAH-contaminated sites, bioremediation is specified by the U.S. Environmental Protection Agency as the preferred remedial technology. Bioremediation of PAH-contaminated soils is often limited, however, by the low solubility of PAH, which inhibits microbial uptake. Adding synthetic surfactants to enhance PAH solubility may be toxic to natural microorganisms and further inhibit bioremediation. Based on results reported here, a potential alternative in unsaturated soil environments may be the application of natural HA to accelerate the biodegradation of PAH.

SR-FTIR spectromicroscopy can assess real-time interactions between multiple constituents in contaminated soils. Combined with conventional mineralization measurements, which monitor respiration through carbon dioxide production, SR-FTIR spectromicroscopy is a powerful tool for evaluating bioremediation options and designing bioremediation strategies for contaminated vadose zone environments.

A longer version of this work will be published in Environmental Science and Technology, 2002.

This work was supported by the Director, Office of Energy Research, Office of Basic Energy Sciences, Materials Science Division, of the U.S. Department of Energy under Contract No. DE-AC03-76SF00098.

Principal investigator: Hoi-Ying N. Holman, Lawrence Berkeley National Laboratory. Email: hyholman@lbl.gov. Telephone: 510-486-5943.

Investigation of Interfacial Chemistry of Microorganisms

Jani C. Ingram,[1] David E. Cummings,[1] Hoi-Ying Holman,[2] and Matthew Downing[3]
[1]Idaho National Energy and Environmental Laboratory, ID
[2]Lawrence Berkeley National Laboratory, CA
[3]Shawnee High School, NJ

INTRODUCTION

Remediation of Department of Energy (DOE) sites contaminated with toxic metals and radionuclides is a complex and costly problem. Several bioremediation strategies currently being explored exploit the metabolism of naturally-occurring dissimilatory metal-reducing bacteria (DMRB). These bacteria catalyze the mobilization of some metal oxide-associated trace elements and the precipitation of many otherwise soluble metals and radionuclides. Our recent work centers on the effects of co-contaminating trace metals on the microbe-mineral interface.

RESULTS

Secondary ion mass spectrometry (SIMS) and synchrotron radiation Fourier transform infrared spectroscopy (SR-FTIR) were applied to examine biochemical changes incurred at the surface of Shewanella putrefaciens cells due to exposure to soluble arsenic. Cells responded to the insult with altered membrane fatty acids (observed by SIMS) and exopolysaccharide production (observed by SR-FTIR).

SR-FTIR at ALS beamline 1.4.3 was used to analyze *S. putrefaciens* cells with and without exposure to 100 mM As(V). The main difference between the spectra of stationary phase cells was the clear lack of a broad peak associated with carbohydrates in the As-exposed cells that was present in the unexposed cells (Figure below). In its place were two distinct peaks indicative of phosphodiester bonds. Phosphodiester bonds are abundant in cell membranes, forming the junction between glycerol and fatty acids. Cell surface carbohydrates likely indicate either a capsule (exopolysaccharides), or common membrane lipids called lipopolysaccharides (LPS). The role of the capsule is especially important in nature, where it can aid the cell in its defense against viruses, hydrophobic toxins such as detergents, and dessication. In addition, it has been implicated in the attachment of some microorganisms to solid substrates. An impaired ability to form exopolysaccharides would likely limit the cells competitive fitness in nature. The LPS may be largely responsible for the net negative charge on the cell surface, implicated in attachment, metal binding, and nutrient transport across the outer membrane. Additionally, the LPS may stabilize the membrane's physical shape and structure. An impaired LPS would also put the cells at a disadvantage in the environment.

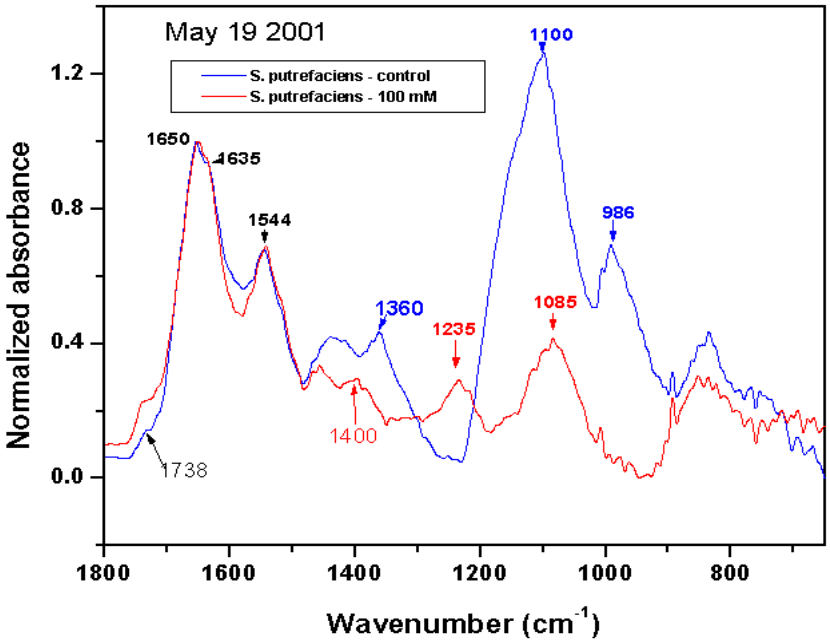

This work was supported by Idaho National Engineering and Environmental Laboratory.

Principal investigator: Jani C. Ingram, Idaho National Engineering & Environmental Laboratory (INEEL), Phone: (208) 526-0739, Fax: (208) 526-8541, email: uoa@inel.gov

New IR microscope and bench installed at BL1.4

Michael C. Martin[a], Hoi-Ying N. Holman[b], and Wayne R. McKinney[a]
[a] Advanced Light Source Division, Lawrence Berkeley National Laboratory, Berkeley, CA 94720
[b] Center for Environmental Biotechnology, Lawrence Berkeley National Laboratory, Berkeley, CA 94720

1. INTRODUCTION

New infrared spectromicroscopy equipment was purchased for and installed on the ALS infrared beamlines on beam port 1.4. It includes the latest step-scan capable FTIR bench and an infinity corrected infrared microscope which will allow for a number of new sample visualization methods. This equipment was purchased with funding from the DOE Office of Biological and Environmental Research (OBER) with the express purpose to develop biomedical and biological applications of synchrotron-based infrared spectromicroscopy.

2. EQUIPMENT

The new spectromicroscopy equipment includes a Thermo Nicolet Nexus 870 step- and rapid-scan FTIR bench, and a Thermo Spectra-Tech Continuum IR microscope, photographed below. The IR microscope includes two IR detectors, a wide-band MCT and a fast (20 ns) TRS MCT for time-resolved experiments. A fast digitizer (up to 100MHz) compliments the TRS MCT detector. The synchrotron beam coupled into the IR microscope continues to have a diffraction-limited spot size, thereby attaining a 200-fold increase in signal from small (3 – 10 micron) sample spot compared to a conventional thermal IR source. The infinity-corrected microscope optics allow for a number of additional sample visualization accessories which can help the user identify the important location within their sample for micro-IR analysis:

- Visual and IR polarizers
- Dark-field illumination
- DIC (Differential Interference Contrast) optics
- UV Fluorescence

An example of DIC optics enhancing a micrograph of human cheek cells is shown in the photograph to the right. The DIC technique provides a psuedo-3D effect, enhancing the contrast between different thicknesses of an otherwise clear sample. In the image to the right, one can make out the nuclei of the cells (thicker bump near the middle of each cell), whereas this would be difficult using conventional illumination.

This new instrument will aide in user scientific research across many fields. For example, the study of individual living cells, toxic contaminants, bioremediation, protein microcrystals, rhizoids, and forensic evidence will all be enhanced by the additional capabilities of this new SR-FTIR spectromicroscopy system.

ACKNOWLEDGEMENTS

This research was supported by the Office of Science, Office of Biological and Environmental Research, Medical Science Division and the Office of Science, Office of Basic Energy Sciences, Materials Sciences Division, of the U.S. Department of Energy under Contract No. DE-AC03-76SF00098 at Lawrence Berkeley National Laboratory.

Principal investigator: Michael C. Martin, Advanced Light Source Division, LBNL, 510-495-2231, MCMartin@lbl.gov

Novel molecular mechanisms of disease susceptibility in plants -- an FTIR study of *Arabidopsis thaliana*

Theodore K. Raab[1], John Vogel[2], Shauna Somerville[1]

[1] Carnegie Institution of Washington, Dept. of Plant Biology,
260 Panama Street, Stanford, CA 94305, USA
[2] University of California, Dept. of Plant Pathology,
Riverside, CA 92521, USA

INTRODUCTION

Understanding the molecular basis of plant resistance to fungal diseases will contribute to reducing world-wide crop losses. One model organism for studying disease resistance is *Arabidopsis thaliana*, a small member of the mustard family for which complete genomic sequence information was publicly released in 2000. *Erysiphe cichoracearum*, the causative agent for powdery mildew disease in a wide range of plants, colonizes and eventually overtakes a host if three events occur. *Erysiphe* spores are carried on the wind, and when they land on the aerial portions of a host plant, they must invade an epidermal (outer) cell, and establish a feeding structure to divert plant nutrients. The fungus must "fly under the radar" of the host's defense responses, which would, if fully activated, quickly kill the invading fungus. Finally, since the fungus is not a saprophytic pathogen (cannot survive on dead tissues), it must keep the host's cells alive until its life cycle is complete. Several genetic loci conferring *p*owdery *m*ildew *r*esistance (*pmr*1-4) have previously been described by Vogel and Somerville [1]. While many disease-resistance pathways involve sensing of salicylic acid and/or jasmonic acid, several genes that operate independently of these hypersensitive responses have been identified; the mutant described below represents a novel form of disease resistance based upon loss of a gene required during a compatible interaction, rather than the action of known host defense pathways.

METHODS

An *Arabidopsis* disease-resistance gene named *PMR*6 has recently been cloned and characterized and encodes a pectate lyase-like enzyme with a novel C-terminal domain [2]. Although the protein has been purified, it has resisted all efforts at demonstrating enzymatic activity towards cell wall polysaccharides. Utilizing Beamline 1.4.3, we undertook a comparative FTIR microscopic study of cleared leaves from wild type (WT) Columbia plants of *Arabidopsis*, as well as plants homozygous for a loss-of-function mutation in *pmr*6. We reasoned that large scale modifications in the pectin component of the cell wall in the mutant compared to wild type should be instructive as to the nature of the molecular lesion. IR spectromicrosopy at BL 1.4.3 allows the chemical characterization of distinct cell types in both living and chemically-cleared tissues at a spatial scale of 6 μm x 10 μm, a significant improvement over thermal IR sources. For these experiments, a few dozen matched seedlings of Columbia WT and *pmr*6-1 were germinated on 1.5% agar plates supplemented with 0.5x MS medium, and cultivated in

growth cabinets at 21^{o} C with {16:8} photoperiod. After 2 weeks, the seedlings were transplanted to a peat:perlite mix supplemented with slow-release fertilizer, and grown an additional 10-12 days in a walk-in growth chamber with continuous light. At the early bolting stage, rosette leaves of both treatments were cleared in 1:1 chloroform:methanol and air-dried flat overnight on microscope slides under sterile cover slips. IR spectra were collected (upon removal of the cover slips) in single-beam reflectance mode at 2 cm^{-1} resolution over the range of 4000 - 650 cm^{-1} (2.5 to 16 micron wavelength) with 512 spectra co-added for Fourier transforms. Spectra were then converted to absorbance basis by ratioing to a gold-coated reflection standard, and small amounts of CO_2 and water vapor subtracted from the spectra. At least a dozen (biological replicates) plants from each class were compared.

For initial data exploration, spectra were converted from Nicolet's OMNIC software controlling the microscopes at BL 1.4.3, to the JCAMP.DX format, and analyzed after area-normalization using **Win DAS** [3], a widely used multivariate statistical package in biotechnology and biospectroscopy. For extremely multivariate data sets such as those produced in FTIR or NMR spectroscopy, the very first step in rational data exploration occurs at the level of dimensional reduction. One such method, principal components analysis (PCA, also known as singular-value decomposition) seeks a new set of m axes (<< r, the number of variates in each spectrum) that projects as much of the variance in the original data as possible. Using a covariance matrix, the software initially calculates a ranking (from increasing to decreasing variance) of the top ten vectors that "span" the original data. In most spectral applications, the first two or three PCs explain much of the difference between the 'treatment' and 'control', often highlighting spectral contributions (known as PC 'loadings' or 'scores') hard to see in the original spectra. Below we discuss two of the products of such an analysis to interpret the molecular distinction between wild type *Arabidopsis* plants and those carrying the disease resistance lesion. It should be kept in mind however, that chemometrics methods are quite general, and can be used, e.g. for interpretation of remote sensing data, as well as DNA microarray experiments in clinical medical settings.

RESULTS

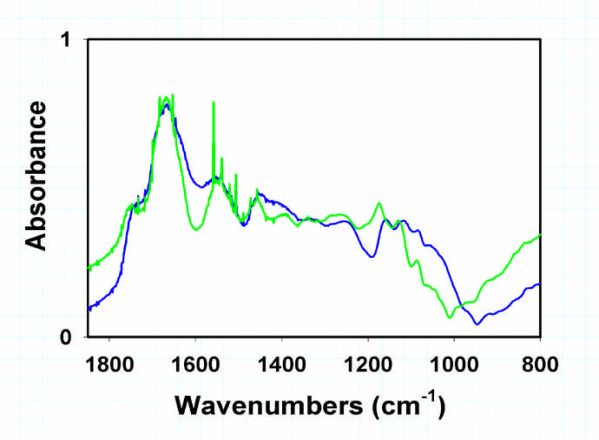

To determine if mutations in PMR6 altered cell wall composition, FTIR spectra were acquired at BL 1.4.3. **Figure 1** compares the mean absorbance spectra of a dozen WT leaves (green) and eighteen *pmr6* leaves (blue) in the carbohydrate 'fingerprint' region from 1800-800 cm^{-1}. Visual inspection of the absorbance spectra from *pmr*6 leaves reveals somewhat greater absorbance in the region attributed to pectin, a major class of cell wall polysaccharides in plants. This is not surprising given that *pmr*6 may be a pectin-degrading enzyme. The absorbance peaks

attributed to cellulose in *pmr*6 cell walls shift down in energy, indicating a greater degree of hydrogen-bonding than WT.

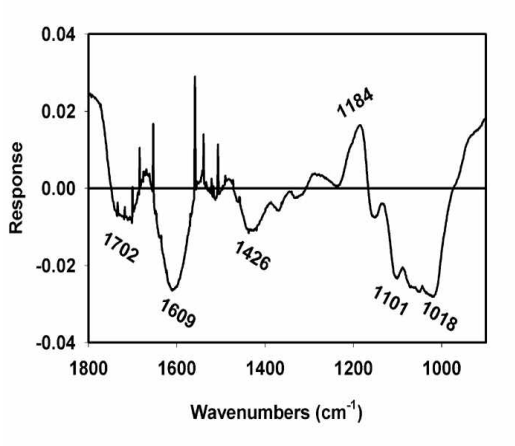

Principal components analysis was employed to identify features that differ between *pmr*6 and wild type, but that are not obvious in the raw spectra. The first three PCs explained 64%, 19% and 9%, respectively of the variation in the full data set. The signature peaks (1609, 1101, 1018 cm^{-1}) of the of the first principal component (**Figure 2A**) points to the enrichment of the of the *pmr*6 cell wall in pectins with a lower degree of esterification and that *pmr*6 cellulose has more intermolecular hydrogen bonds (1426 cm^{-1}) than WT. The 2nd PC (not shown) corresponded to higher levels of protein in the *pmr*6 leaves relative to WT. The statistical separation of the two types of *Arabidopsis* plants can be seen in the biplot of **Figure 2B**.

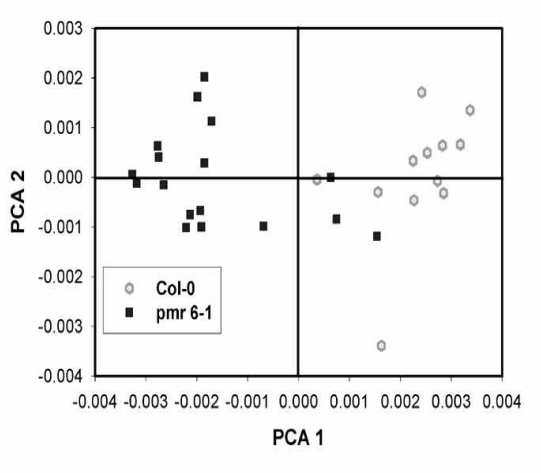

Spectroscopic observation of the altered pectin composition of the cell wall fits well with the possible pectin-degrading/binding activity for the *PMR6* gene. The alterations of seen by FTIR in *pmr*6 cell wall composition may have made the plants less palatable to the pathogen *Erysiphe* spp. We are at work to identify other actors in this pathway and to interpret changes in cell wall composition by various IR techniques at the ALS.

REFERENCES

1. J. Vogel and S. Somerville, "Isolation and characterization of powdery mildew-resistant *Arabidopsis* mutants," Proc. Natl. Acad. Sci. USA **97**, 1897-1902 (2000).
2. J. Vogel, T.K. Raab, C. Schiff, S. Somerville, "PMR6, a pectate lyase-like gene required for powdery mildew susceptibility in *Arabidopsis*," Plant Cell (in review, 2002).
3. E.K. Kemsley, *Discriminant analysis and class modeling of spectroscopic data*. (John Wiley and Sons, 1998).

T.K.R. was supported by a Carnegie Fellowship during these experiments, and J.V. was supported by an NIH Fellowship F32 GN19499-01 while at Carnegie. Additional support was received from the U.S. Department of Energy, Biological Energy Research Program and by Novartis Crop Protection AG.

Principal Investigator: Dr. Theodore K. Raab, Carnegie Inst. of Washington, Dept. of Plant Biology, 260 Panama St., Stanford CA 94305. Email: tkraab@Andrew2.Stanford.edu. Telephone: 650-325-1521 ext. 446.

Spatial Distribution of Bacteria on Basalt Using SR-FTIR

Mary E. Kauffman,[†,1,2] Hoi-Ying Holman,[3] R. Michael Lehman,[2] Michael C. Martin[4]

[1]Idaho State University, Depts. Of Biologiy and Geology, Pocatello, ID, 83209, [2]Idaho National Engineering and Environmental Laboratory (INEEL), Idaho Falls, ID, 83415, [3]Center for Environmental Biotechnology, Lawrence Berkeley National Laboratory, Berkeley, CA, 94720, [4]Advanced Light Source, Lawrence Berkeley National Laboratory, Berkeley, CA, 94720. [†]Address correspondence to Mary E. Kauffman, INEEL, Geomicrobiology Group, PO Box 1625, MS 2203, Idaho Falls, ID, 83415. Email:kaufme@inel.gov

INTRODUCTION

Understanding the role of microorganisms on the fate and transport of contaminants is essential in the determination of risk assessment and the development of effective remediation strategies for contaminated sites. The microscale distribution of microorganisms on the surface of complex geologic media will affect the types and rates of biotransformations in contaminated environmental systems. In this study, we used synchrotron radiation-based Fourier transform infrared spectromicroscopy (SR-FTIR) at the Advanced Light Source (ALS) Beamline 1.4.3, Lawrence Berkeley National Laboratory (LBNL), to investigate the preferential attachment of *Burkholderia cepacia* G4 to the various mineral phases within basalt. SR-FTIR is a non-destructive, in situ analytical tool, that when coupled to an automated X, Y positioning stage, can provide surface mapping of biochemical functional groups.

MINERAL AND BASALT SPECIMENS

Basalt specimens were prepared from core samples. The center of the core was cut into 1” square blocks and then sliced into specimens 1 mm thick using a diamond saw blade and water as the lubricant. Mineral standards for the four major mineral phases in basalt (plagioclase, augite, ilmenite and olivine) were prepared in the same fashion. The specimens were sonicated and autoclaved prior to use. Basalt and mineral specimens were spectrally characterized using SR-FTIR prior to, and after, exposure to a bacterial growth culture for several days. SR-FTIR spectra

of the distinct mineral phases in the basalt were compared to spectra obtained for individual mineral standards.

BACTERIAL CELLS, CULTURES AND CONDITIONS

Burkholderia cepacia G4 was selected as the model organism for this study due to the fact that it is a common soil microorganism, and therefore representative of bacteria found in environmental systems. Microcosms consisting of basalt or mineral specimens and bacterial culture solution were placed on a rotary shaker (55 rpm) at 23 ° C for five days. The culture solutions were changed daily and new inoculum was added. At the end of the five days, the specimens were removed from solution and rinsed with phosphate buffer to remove any loose cells.

SR-FTIR SPECTROMICROSCOPY

SR-FTIR spectra were collected at Beamline 1.4.3 at the ALS, LBNL, Berkeley, CA. All SR-FTIR spectra were recorded in the 4000-650 cm^{-1} infrared region. This region contains absorbance features correlative to characteristic IR-active vibrational modes for common biomolecules such as nucleic acids, proteins and lipids, as well as identifying absorbance features for the basalt and mineral specimens. Spectral maps of the basalt surfaces were obtained by programming the microscope X-Y positioning stage to collect spectra at specific step locations and then extracting spatial information of functional groups based upon absorbance peak wavenumbers. Data was collected in single-beam reflectance mode with a spectral resolution of 4 $cm^{-1}$and 64 scans were co-added for Fourier transform processing for each spectrum. Each resulting spectrum was then ratioed to the spectrum of a gold slide to produce absorbance values. By extracting each individual spectrum within the mapping grid and comparing it to spectra collected on each of the four individual minerals, identification of the underlying mineralogy can be determined. Figure 1 shows the spatial distribution of bacteria on a basalt surface, based upon the occurrence of the protein amide I peak at ~1650 cm^{-1}, and the preferential attachment by *B. cepacia* G4 to plagioclase. The total map area was 250 X 105 μm

with spectra collected every 25 µm along the X coordinate and every 15 µm along the Y coordinate. Correlative maps of the same surface area were constructed based upon the protein amide II peak at ~1550 cm^{-1} and at least one other absorbance feature related to the presence of biomolecules, to insure the resulting map was due to the spatial distribution of bacteria and not an artifact of the mineralogy (data not shown).

RESULTS

Multiple SR-FTIR maps of basalt surfaces colonized by bacterial cultures showed preferential attachment by *B. cepacia* G4 to plagioclase within the basalt matrix. The mineral apatite ($Ca_5(PO_4)_3(F, Cl, OH)$) is a common accessory mineral in igneous rocks and appears as inclusions in igneous plagioclase feldspars. Phosphorous is required by bacterial cells for the synthesis of nucleic acids and phospholipids. Scanning electron microprobe results indicate the presence of phosphorous in both the plagioclase within the basalt matrix and in the Ward's standard plagioclase specimen (data not shown). A recent study on feldspars as a source of nutrients determined that microorganisms extracted inorganic phosphorous from apatite inclusions in alkaline feldspars. It is highly likely that *B. cepacia* G4 preferentially attaches to the calcic plagioclase in order to access phosphorous from apatite inclusions.

This work was supported by the Idaho National Engineering and Environmental Laboratory.

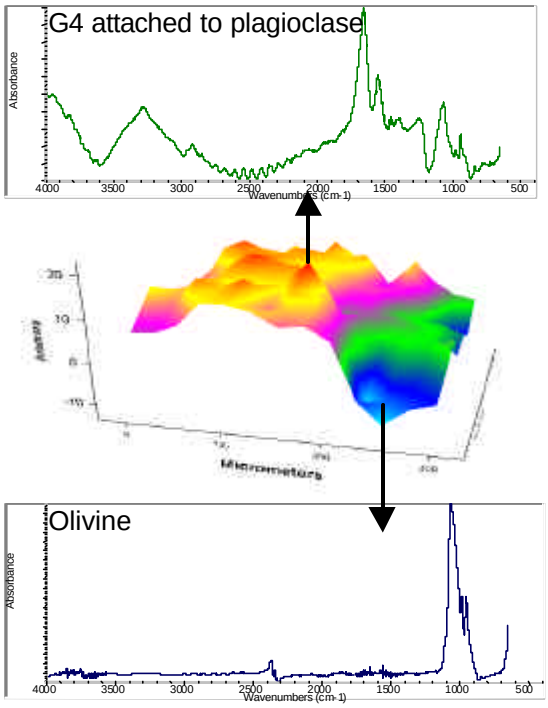

Figure 1.

SR-FTIR Study of Bacteria-Water Interactions: Acid-base Titration and Silification Experiments

Nathan Yee[1], Liane G. Benning[1], Mark J. Tobin[2], and Kurt O. Konhauser[1]

[1]School of Earth Sciences, University of Leeds, United Kingdom
[2]Synchrotron Radiation Source, Daresbury Laboratory, United Kingdom

Bacterial surfaces are highly reactive and can strongly affect mass transport in a wide range of geological environments. Bacterial cell walls can adsorb aqueous metal cations, and can act as nucleation surfaces for heterogeneous mineral precipitation. However, the reactions at the bacteria-water interface are poorly understood, primarily due to the difficulty in monitoring such processes *in situ* and *in vivo*. In this study, we use synchrotron radiation-based FTIR to investigate the chemistry of bacterial surfaces with acid/base titration and Si precipitation experiments. The objectives of this research are to identify the reactive surface functional groups and to determine how metal adsorption/precipitation affects the protein and lipid structures of individual living bacterial cells. *In-situ* FTIR experiments were performed on the Infrared beamline 1.4.3 at the Advance Light Source (Lawrence Berkeley National Laboratory), using a Nicolet 760 FTIR bench and a Spectra-Tech Nic-Plan IR microscope. All experiments were performed with flow through fluid cell with BaF_2 and ZnSe windows separated by a 6 um mylar spacer. Acid-base titration and Si precipitation experiments were conducted with both intact cells and isolated bacterial sheaths of *Calothrix* (strain KC97) a filamentous cyanobacteria. Titration experiments with intact bacterial cells show a change in peak position of the carboxylic functional group at ~1400 cm^{-1} (symmetric vibrational stretching of deprotonated carboxylate groups) from acidic to near-neutral pH (Fig 1). The bacterial silicification experiments indicate a change in peak position at ~ 1700 - 1740 cm^{-1}, corresponding to the vibrational C=O stretching of esters groups in the lipid structures of the cell (Fig 2). Previous studies have demonstrated that hydrogen bonding onto carbonyl functional

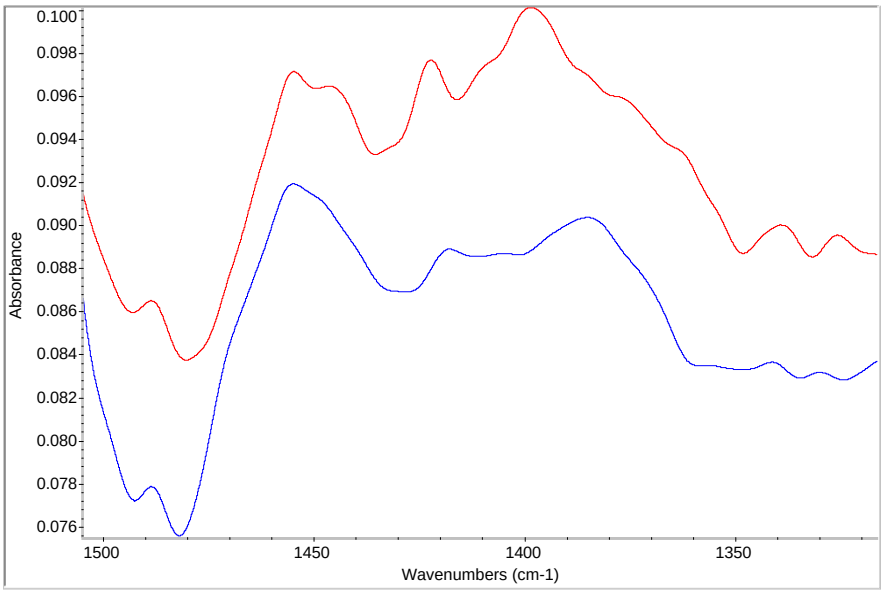

Figure 1. Infrared spectra of an intact *Calothrix* cell in aqueous solution at pH 2.9 and 6.3. A shift in peak position is observed at 1400 cm^{-1} corresponding to $\nu_s(COO^-)$ stretching of deprotonated carboxylate functional groups.

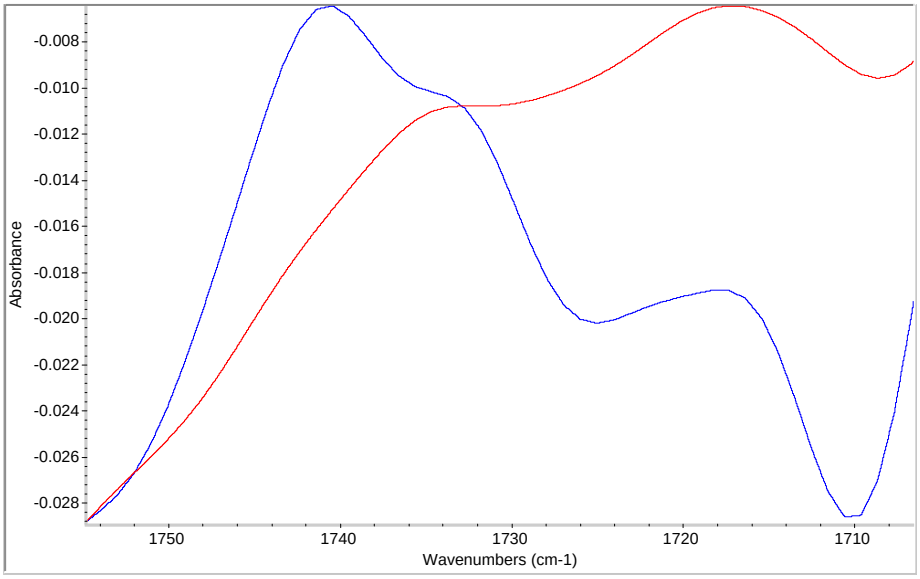

Figure 2. Infrared spectra of an intact *Calothrix* cell before and after silicification. A change in peak position of vibrational C=O stretching is observed.

groups can shift the peak positions in this wavenumber range. Finally, infrared microspectrometry experiments were performed to image the proteins, lipids, and nucleic acids inside intact living cells. Spatial resolution of a few microns was achieved and the chemical distribution of proteins was mapped throughout a *Calothrix* filament (Fig 3). The data indicate that protein molecules have a high concentration within the cell, but a very low concentration on the bacterial surface. These results demonstrate that SR-FTIR can be applied to investigate the functional group chemistry of bacteria in a range of different bacteria-water systems.

This work is an ENVIROSYNC project funded by the Natural Environmental Research Council, UK.

Principal investigator: Liane Benning, University of Leeds, +44-113-233-5220, liane@earth.leeds.ac.uk.

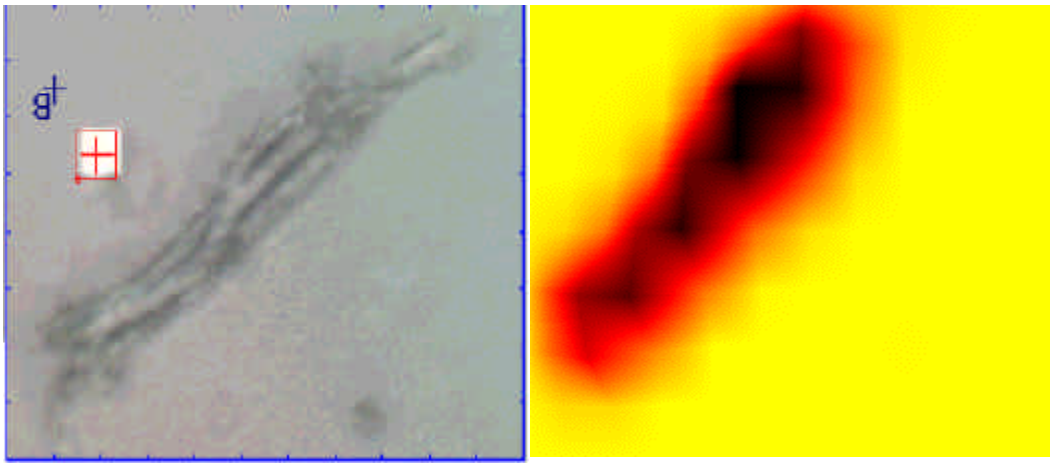

Figure 3. Chemical distribution of the protein characteristic bands amide I and amide II (1495-1800cm^{-1}) of a *Calothrix* filament. a) Optical image, b) 2-D map of the protein distribution.

Synchrotron Infrared Spectromicroscopy as a Novel Bioanalytical Microprobe for Individual Living Cells: Cytotoxicity Considerations

Hoi-Ying N. Holman,[*] Kathleen A. Bjornstad,[†] Morgan P. McNamara,[†]
Michael C. Martin,[‡] Wayne R. McKinney,[‡] and Eleanor A. Blakely[†]
[*]Center for Environmental Biotechnology, [†]Life Sciences Division, [‡]Advanced Light Source Division,
Lawrence Berkeley National Lab, Berkeley, CA, 94720

INTRODUCTION

Recent progress in analytical instrumentation has enabled dramatic advances in gene sequencing and protein identification techniques. Using the information produced by these techniques, the attention of biomedical researchers is now increasingly focused on understanding how chemical species interact in living organisms by the use of imaging techniques that simultaneously provide morphological and chemical information within cells and tissues. Most imaging research has focused on fluorescent labeling to locate a specific chemical event within the cell. However, bond breaking, ionization, and other damage has been shown to occur during excitation with UV, visible, and even the more recent near-IR two-photon techniques.

In contrast, synchrotron-based Fourier transform infrared (SR-FTIR) spectromicroscopy has the ability to monitor the chemistry within an individual living cell without labels and with even lower photon energies. Combining SR-FTIR spectroscopy with microscopy yields a powerful tool for non-destructively probing bio-systems on a small size scale. The sample can be small and/or heterogeneous, for example; individual living cells, microorganisms, and larger biological systems in which local biochemistry may have significant spatial variations.

It is crucial to know if the synchrotron radiation-based mid-infrared (SR-IR) source causes any short- or long-term effects on the living biological samples under study. Mid-infrared photons are significantly lower in energy (0.05 – 0.5 eV) than excitation sources used for fluorescence, implying that photo-induced effects will be minimal. However, to be assured that the SR-IR beam does not perturb living samples via other mechanisms, more detailed studies are required. We recently measured that sample heating from the synchrotron IR beam is minimal (~ 0.5°C).

Here we present the results of in vitro studies to determine if the SR-IR beam causes any detectable immediate or long-term cytotoxic effects on living cells. Four widely accepted assays were used to look for deleterious effects on cells subjected to the SR-IR beam.

MATERIALS AND METHODS

The studies used a human T-1 cell-line from an established aneuploid cell-line derived from human kidney tissue. They were maintained in a standard growth medium at pH 7.4. Cells were grown at 37°C in a humidified atmosphere of 5% CO_2 and 95% air. Cells were sub-cultured every 3-4 days. T-1 cultures were grown to confluence to ensure para-synchronization. Fluorescence-activated Cell Sorting (FACS) analysis demonstrated that 85% of the cells in these cultures were synchronized to G0/G1 phases. A custom on-stage mini-incubator was used to maintain the proper moisture and growth environment for the cells while allowing *in situ* FTIR spectromicroscopy measurements. Selected cells were exposed at 37°C to the focused synchrotron infrared beam for a specified duration of 5, 10, or 20 minutes. Once completed, fresh growth media was replaced on the dish and it was returned to the standard incubator.

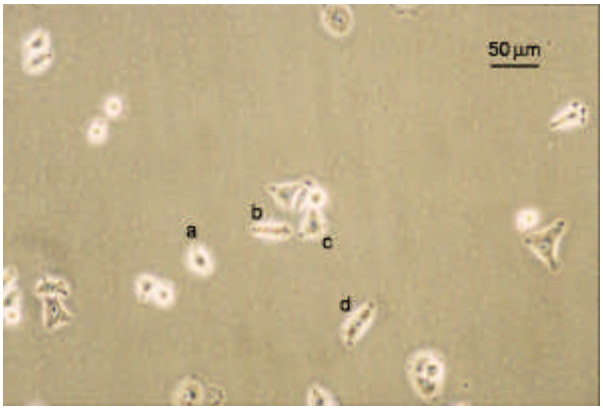

Figure 1. Photograph showing results from alcian blue assays of cells exposed to the SR-IR beam for (a) 5, (b and c) 10, and (d) 20 minutes. Other cells were not exposed and were negative controls. No cells show retention of the blue dye demonstrating that no immediate cytotoxicity is observed.

Negative controls were non-exposed cells located in the same field (internal controls), and therefore experienced the same handling. Positive controls were cells killed by either a 70% alcohol solution or dehydration.

RESULTS AND DISCUSSION

Figures 1-4 show representative photographs for each assay. In no case did we find a result differing with the representative ones shown.

SR-IR beam has no short-term effect on cell viability. Alcian blue assays were carried out as shown in Figure 1. Neither cells exposed to up to 20 minutes of synchrotron IR beam nor nearby non-exposed cells retained the blue dye 6 hours after exposure. This indicates that the SR-IR beam did not produce detectable effects on the viability of exposed cells. Other exposed cells remained free of stain 12 and 24 hours after exposure indicating that their membranes still remained intact. In contrast, dead positive control cells were stained blue as expected, as their membranes had become permeable to the dye molecules.

Cells survive and continue to proliferate days post exposure. The long-term colony-forming assay demonstrates that the exposed cells also continue to proliferate into colonies. The exposed test cells and nearby non-exposed cells proliferated into colonies of similar size (Figure 2), well over fifty cells in ten days. The positive control cells, on the contrary, had detached from the petri dish and disappeared from the field. Since none of the 46 SR-IR exposed test cells developed into colonies with less than 50 cells, we interpret this as an indication that SR-IR beam does not impact cell survival and proliferative activities.

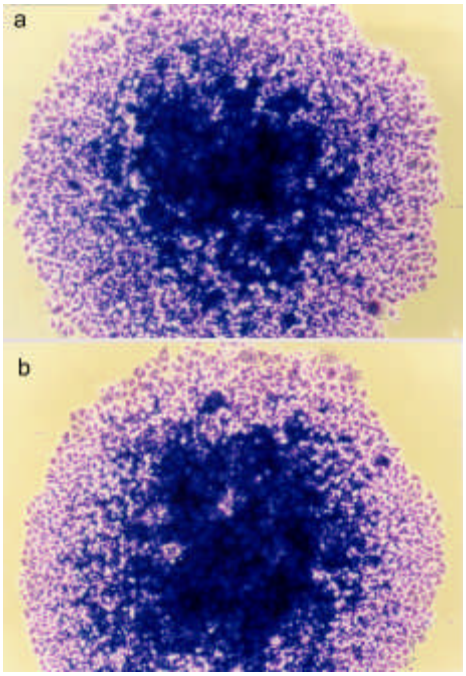

Figure 2. Colony forming from (a) a negative control cell and (b) a test cell exposed to the SR-IR beam for 20 minutes. Both cells proliferated into similar sized colonies after 10 days.

Exposure to SR-IR does not compromise cell-cycle progression. Cell-cycle progression in exposed cells were monitored by the incorporation of BrdU into newly synthesized DNA at 11 hours after cell setup and 10 hours post SR-IR exposure. Both exposed cells and non-exposed controls had reached the DNA synthetic phase (S-phase) of cell- cycle at this 12-hour observation point (Figure 3). The similarities among these immunofluorescent staining of BrdU (and DAPI) labeled cells indicate that the exposed cells are not compromised in their ability to enter their S-phase in the cell cycle after exposure to the SR-IR beam. Furthermore, the lack of BrdU uptake in exposed and control cells at 6 or 24 hours demonstrates that the cell-cycle

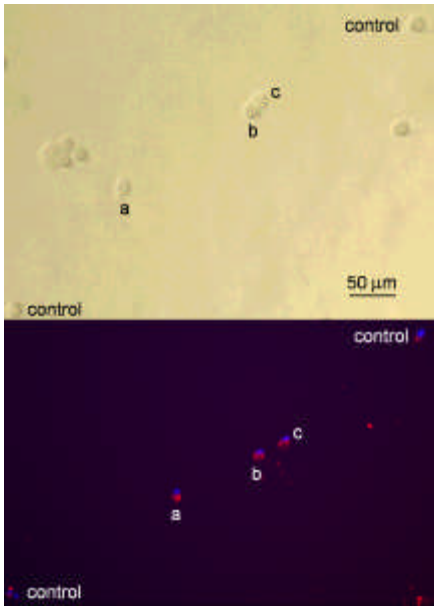

Figure 3. BrdU assay results for cells exposed to the SR-IR beam for (a) 5, (b) 10, and (c) 20 minutes. Two other cells in the field were unexposed and used as negative controls. In the lower panel, blue indicates DNA and red indicates BrdU incorporation during DNA synthesis. All cells show the same incorporation of BrdU into the DNA.

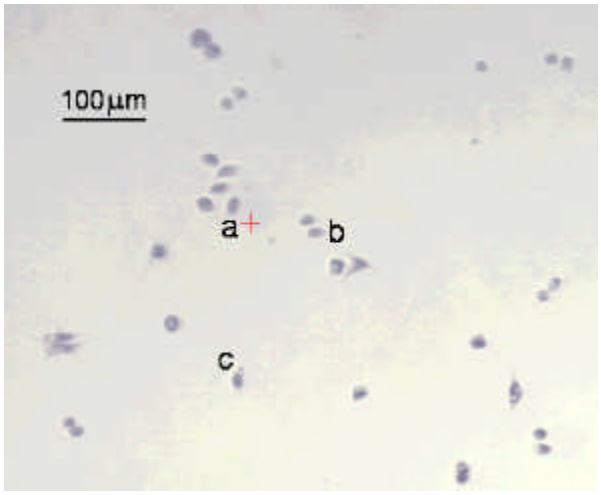

Figure 4. MTT assay results for cells that had been exposed to the SR-IR beam for (a) 5, (b) 10, and (c) 20 minutes. Other cells in the field were unexposed and used as controls. All test and control cells show the same blue color indicating the same level of metabolic activity.

progression of SR-IR exposed cells remains uninterrupted.

ATP and NAD+-associated metabolic activity is not impaired by the SR-IR beam. A two-hour MTT assay was carried out and representative photos of the results are shown in Figure 4. Cells exposed for 20 minutes and nearby non-exposed controls show similar purple-blue stain. On the contrary, tetrazolium salt solution remained yellow in the killed (positive) controls with no purple-blue stain uptake. Results were identical for 5- and 10-minute exposures. This implies that both the exposed and negative control cells produced mitochondrial dehydrogenases during the two-hour MTT assay. Mitochondrial dehydrogenases are associated with the ubiquitous metabolic pathway of glycolysis that generates the critical biomolecules of ATP and NAD+. These results indicate that the SR-IR beam has negligible effects on this important metabolic pathway which provides energy to cells.

In all 4 assays studied we found no detectable changes between cells exposed to the synchrotron infrared beam and nearby non-exposed controls. 267 individual cells were tested with zero showing measurable cytotoxic effects (counting statistics error is 6.1%), with over 1000 control cells used. These results show that the high-brightness mid-IR synchrotron beam is not only non-destructive, but also causes no effects on both the short- and long-term viability, proliferation, and metabolism within living human cells. The results reported here lay an important foundation for future biomedical and biological applications of synchrotron infrared spectromicroscopy, which will complement other biochemistry and microscopy techniques.

This research was supported by the Office of Science, Office of Biological and Environmental Research, Medical Science Division and the Office of Science, Office of Basic Energy Sciences, Materials Sciences Division, of the U.S. Department of Energy under Contract No. DE-AC03-76SF00098 at Lawrence Berkeley National Laboratory.

Principal investigator: Hoi-Ying N. Holman, Lawrence Berkeley National Laboratory. Email: hyholman@lbl.gov. Telephone: 510-486-5943.